

## Synthesis and Characterization of Nanostructured Tungsten Trioxide (WO<sub>3</sub>) Thin Films

Fatma Badry Mohamed<sup>1,2\*</sup>, Badr Mohamed Ali<sup>1,2</sup>, Reda Mohamed Nageib<sup>1,2</sup>,  
Haroun Abd El-Fatah Elshaikh<sup>1,2</sup>

<sup>1</sup>Department of Physics, Faculty of Science, Aswan University, Aswan, Egypt.

<sup>2</sup>Research Center for NanoMaterial Studies and Their Promising Technologies, Aswan, Egypt.

Received: 25/7/2020

Accepted: 13/8/2020

© Unit of Environmental Studies and Development, Aswan University

### Abstract:

Tungsten trioxide (WO<sub>3</sub>) has attracted great attention due to its promising and wonderful properties. In this study, the influences of calcined temperature on the structural, morphological and optical properties of WO<sub>3</sub> were investigated. Sodium tungstate dehydrates (Na<sub>2</sub>WO<sub>4</sub>·2H<sub>2</sub>O, 99.9%) powder was used as starting precursor. A sol-gel spin coating technique was used to synthesize pure WO<sub>3</sub> thin films. The as-deposited films have been annealed at 300 °C, 400 °C, 500 °C, 550 °C and 600 °C for 2 hours. The structural properties of thin film samples have been studied by the X-ray diffractometer (XRD) with Cu K $\alpha$  radiation of wavelength 1.542 Å. X-ray diffraction data has been used to find out changes in the crystallite size and to determine the phases present in the films. Field emission-scanning electron microscopy (FE-SEM) has been performed to investigate the surface morphology of the prepared samples. The optical band gap energy of the thin films has been investigated and analyzed using UV-Vis spectrophotometer equipped with an integrating sphere and a Spectral reflectance standard. The absorbance of the films was measured in a wavelength range of 190–2500 nm. From the results it was found that the characterized peaks were associated to the crystalline planes of the monoclinic phase of WO<sub>3</sub>. The crystallite sizes increased with increasing calcination temperatures. It was observed that the WO<sub>3</sub> had a sphere-like structure composed of numerous nanoparticles. The absorbance spectra show that there is a red shift in the absorption edge as the calcined temperature increases. The optical energy gap was decreased as the calcined temperature increased. The estimated energy gap values for the thin film sample under consideration was about 2.95, 2.58, and 2.023 for samples calcined at 400 °C, 500 °C, and 550 °C respectively.

**Keywords:** NanoWO<sub>3</sub> ; thin films; spin coating technique; optical; morphological properties.

---

**Corresponding authors\*:** E-mail addresses: [fatmaowny@sci.aswu.edu.eg](mailto:fatmaowny@sci.aswu.edu.eg)

## 1. INTRODUCTION

The oxides of transition metals such as tungsten trioxide ( $\text{WO}_3$ ) are very important for the development of many functional materials and smart devices because of its chemical stability, low cost, non-toxicity, semiconducting, electrochemical and optoelectronic properties (Chen et al., 2016; Pal et al., 2018). Tungsten trioxide ( $\text{WO}_3$ ) is n-type semiconductor that have band gap of  $\sim 2.8$  eV, and it exhibits various crystallographic phases including hexagonal, monoclinic, orthorhombic and cubic (Chacón et al., 2015). Tungsten trioxide ( $\text{WO}_3$ ) is feasible electrochromic materials which can be applied for many potential utilizations due to their high optical reversible color change induced by electrochemical process. That lead to wide range applications in electrochromic devices (Deepa et al., 2006), gas sensors (Boulova et al., 2001; Kanan and Tripp, 2007; Liu et al., 2009; Su et al., 2010; Wang et al., 2010), electrochemical capacitors (Chang et al., 2011), optical devices (Ozkan et al., 2002), photo catalysts (Sun et al., 2009), and smart windows (Su and Lu, 1998).

Many methods have been reported for the synthesis of  $\text{WO}_3$  nanostructures, such as sputtering (Garg et al. 2005), chemical vapor deposition (Joraid, 2009), pulsed spray pyrolysis (Patil et al., 2005), sol-gel route (Işık et al., 2009) and Spin Coating Technique (Çırak et al., 2006). Riech et al. (2013) have proposed the synthesis of  $\text{WO}_3$  thin films by using a sol gel spin coating deposition method.  $\text{WO}_3$  films were prepared by using spin coating and screen printing method in the presence of organic additive such as polyvinylpyrrolidone (Go et al., 2016). Saleem et al. (2015) have successfully prepared  $\text{WO}_3$  thin films using Thermal evaporation method.

In this study, the effect of calcined temperature on the deposition of pure  $\text{WO}_3$  thin films based on sol-gel spin coating technique will be examined. The structural properties, surface morphologies and the optical properties of the films will be investigated by mean of X-ray diffractometer (XRD), field emission- scanning electron microscope (FE-SEM) and UV-Vis spectrophotometer respectively.

## 2- MATERIALS AND METHODS

### 2.1- Chemicals and Reagents:

Sodium tungstate dehydrates ( $\text{Na}_2\text{WO}_4 \cdot 2\text{H}_2\text{O}$ , 99.9999%) powder was used as the starting precursor for sol-gel synthesis of nanostructured Tungsten trioxide ( $\text{WO}_3$ ). Hydrogen peroxide  $\text{H}_2\text{O}_2$  (99.999%), hydrochloric acid HCL (37%) and concentrated ammonium hydroxide  $\text{NH}_4\text{OH}$  (33% reagent, 99.99% purity ACS) were bought from DOP ORGANİK KİMYA SANAYİ VE TİCARET LİMİTED ŞİRKETİ. All the chemical and reagents were used as received without further purification. During all the experiments, deionized water (DI) with electrical resistivity of  $18.2 \text{ M}\Omega \text{ cm}$  at  $25^\circ \text{C}$  was used for solution preparation and washing steps.

### 2.2- Preparation Procedure:

A simple sol-gel route was used to synthesize pure  $\text{WO}_3$  thin films. The precursor solution used for deposition of the films was prepared by dissolving desired amount (1g) of  $\text{Na}_2\text{WO}_4 \cdot 2\text{H}_2\text{O}$  in (15ml) deionized water and stirring with the aids of Hotplate Stirrer (MSH-20A, Wise Stir) at

room temperature until complete dissolution was achieved. Hydrochloric acid (HCl) was added drop wise to the precursor solution without stirring until the solution becomes acidic. The precipitation was washed many times by decantation. Decanting the clear solution is better than the filtration route. Next, a mixture of H<sub>2</sub>O<sub>2</sub> and H<sub>2</sub>O (molar ratio of 1:1) was added to the precipitate under intense stirring and heating. Subsequently, small amount of NH<sub>4</sub>OH was added into the solution under intense stirring and heating. Finally, the precipitate was dissolved and a transparent solution was obtained.

For the fabrication of the films, the glass substrate was cleaned with deionized water and dried at 100 °C for 10 min, before the deposition processes. Next the transparent solution was deposited on cleaning substrates by the spin-coating method. The rotation speed was fixed on 2500 rpm/30 sec. The films were dried at 150 °C for 15 min. This drying procedure stabilizes the films. Finally, Nanostructured thin films of crystalline WO<sub>3</sub> were obtained by calcination of the result films at 300 °C, 400 °C, 500 °C, 550°C and 600 °C. All the steps of the calcination process were carried out for 2 h with a heating or cooling rate of 5 °C /min.

### **2.3- Characterization Techniques**

The existed phases and the crystalline structure of the thin film samples were identified by X-ray diffractometer (Bruker: Model AXS- D8 Advance, Germany) with operating conditions, an accelerating voltage of 40 kV and applied current of 40 mA with Cu-K $\alpha$  radiation of wavelength ( $\lambda$ ) = 1.541838 Å. XRD data was recorded for the diffraction angles ( $2\theta$ ) which ranging from 10° up to 70° with a step of 0.16°. The crystallographic databases of Powder Diffraction File (JCPDS) were used for the phase identification of the nanostructured thin films.

Field Emission- Scanning Electron Microscopy (FE-SEM) (FE-SEM, QUANTAFEG250, Netherland) was used to observe the surface morphology of the thin film sample.

The absorbance spectroscopy of the thin films was performed using UV-Vis JASCO: V-670 double beam spectrophotometer with an extending Spectral Range from 190 to 2500 nm, wavelength scanning speed variation from 10 to 8000 nm/min, Spectral Band width variation ranging from 0.1 to 10 nm and Data Interval (data pitch) variation extending from 0.025 to 5 nm.

## **3- RESULTS AND DISCUSSION**

The XRD patterns of the prepared WO<sub>3</sub> thin films at different calcination temperatures are shown in Fig. 2. The crystalline planes were identified using JCPDS monoclinic card No. 04-019-8982 with lattice constants ( $a = 5.2557$  Å,  $b = 5.0986$  Å, and  $c = 7.6242$  Å). The narrow peaks and good intensity have indicated the presence of the obtained WO<sub>3</sub>. In the XRD pattern for WO<sub>3</sub> thin films calcined at 300°C shows one diffraction peak observed at  $2\theta = 41.74^\circ$ , that associated to the (121) crystalline planes of the monoclinic phase of WO<sub>3</sub>. The XRD pattern for WO<sub>3</sub> calcined at 400 °C, 500 °C, 550 °C and 600 °C shows two dominant crystalline plane orientations: (002) at  $2\theta = 23.22^\circ$  and (-112) at  $2\theta = 32.7^\circ$ .

The crystallites size is important parameter which influences the nanostructures properties of metal oxide. The crystallite sizes of prepared thin films were calculated using the Scherrer's equation:

$$D = 0.9 \lambda / B \cos (\theta) \quad (1)$$

where D is the crystallite size (nm),  $\lambda$  is the wavelength of the X-ray radiation,  $\theta$  is the Bragg's angle and B is the full width at half maximum (FWHM) of the peak at  $2\theta$ .

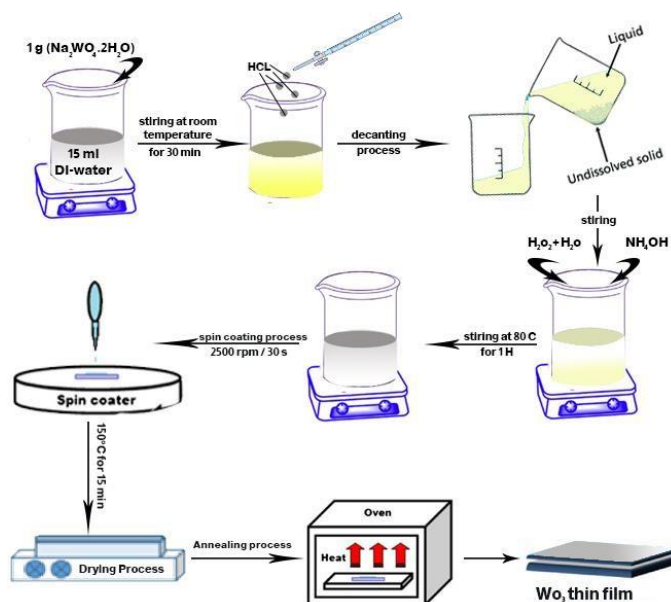


Fig 1. Schematic presentation of  $WO_3$  thin films preparation.

Table 1 Crystallite sizes of pure  $WO_3$  nanomaterial after calcination at different temperatures.

Calcination temperature(°C)	Peak position (°)	hkl	FWHM (°)	Crystallite size (nm)
300	41.74	121	0.96	10.18
	16.5	100	0.3425	24.155
500	27.32	111	0.36571	13.279
	41.58	121	0.423	6.63
550	16.46	100	0.3095	14.861
	23.86	002	0.325	24.98
	27.28	111	0.447	19.625
600	16.54	100	0.241	26.15
	23.4	002	0.234	29.288
	27.34	111	0.234	26.807

The crystallite sizes of the  $WO_3$  thin films synthesized at different calcination temperatures are listed in table 1. It can be seen that the crystallite sizes increased as calcination temperature increased. Analogous behavior and results were obtained by Wang et al.(2003) , they found that the crystallite sizes increased with increasing calcination temperatures from 350°C, 450°C, 550°C to 650°C the crystalline sizes were 9.3, 16.4, 17.1 and 30 nm , respectively. On the other hand, Susanti et al.(2012) found that the crystalline sizes were 7.31, 9.92, 20.4 and 28.36 nm when the calcination temperatures increased from 300°C, 400°C, 500°C to 600°C.

Field Emission- Scanning Electron Microscopy was used to observe the morphology of the thin film sample calcined at 600°C. It can be observed that the WO<sub>3</sub> had a sphere-like structure composed of numerous nanoparticles.

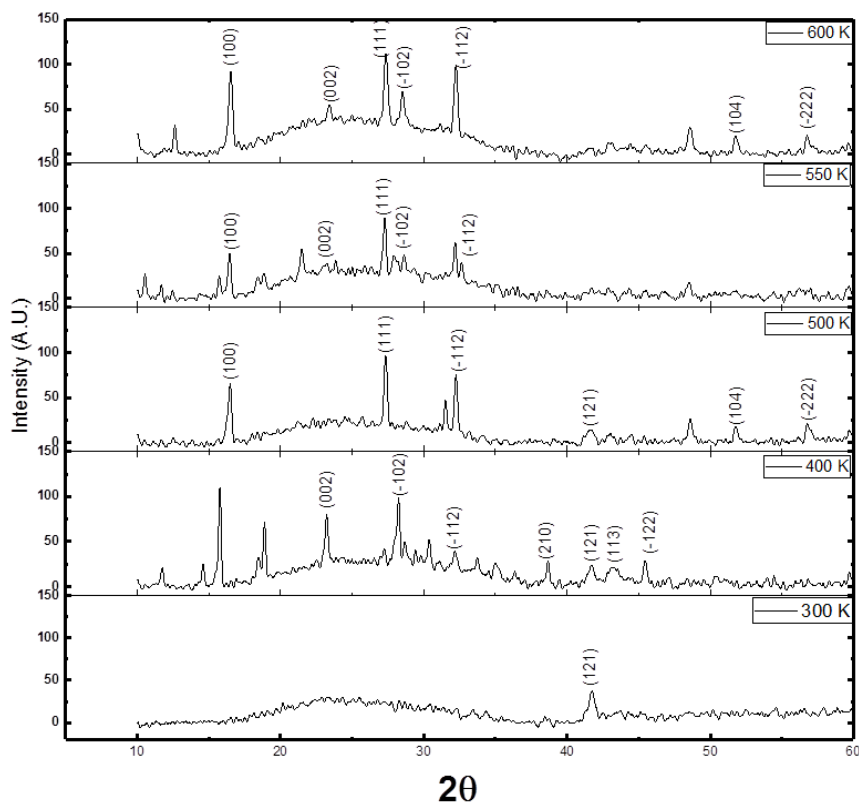


Fig.2 XRD patterns of WO<sub>3</sub> thin film calcined at 300 °C, 400 °C, 500 °C, 550 °C and 600 °C.

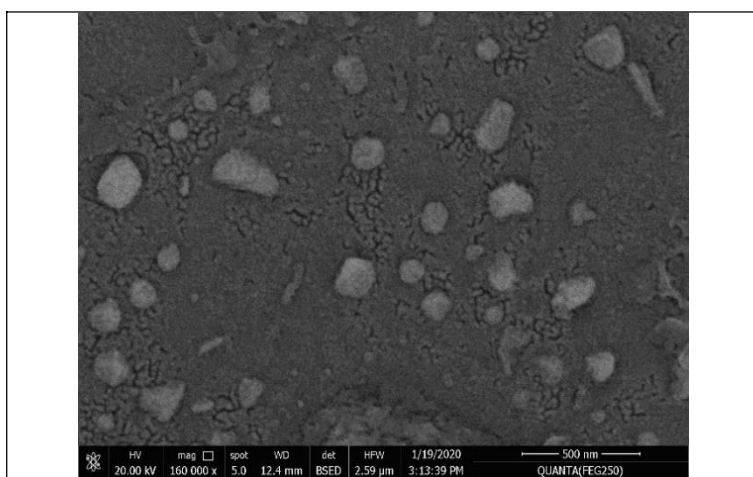


Fig. 3 FE-SEM images for WO<sub>3</sub> thin film calcined at 600 °C.

The absorbance spectra for the samples calcined at 300 °C, 400 °C, 500 °C and 550 °C was reported in figure 4. It can be shown that further increase in the calcination temperature the

absorbance increase. Also it can be seen that there is a red shift in the absorption edge as the calcined temperature increases, due to a reasonable increase in crystallite size.

The optical energy gap  $E_g$  (eV) for the thin film samples have been calculated using the following equation:

$$\alpha h\nu = A(h\nu - E_g)^2 \quad (2)$$

A is the slope of Tauc edge. Thus, Tauc's plots of  $(\alpha h\nu)^2$  versus  $(h\nu)$  should be linear and extrapolate to value of optical gap,  $E_g$ .

The band-gap ( $E_g$ ) determined from Tauc plot as shown in Fig. 4-b, showing a decrease with increasing calcination temperature, this may due to increased crystallite size. The energy gap values for the thin film sample calcined at 400 °C is about 2.95 generally consistent with that reported for the  $WO_3$  ( $E_g=2.8$  eV), and it was 2.58, and 2.023 for samples calcined at 500 °C, 550 °C, respectively.

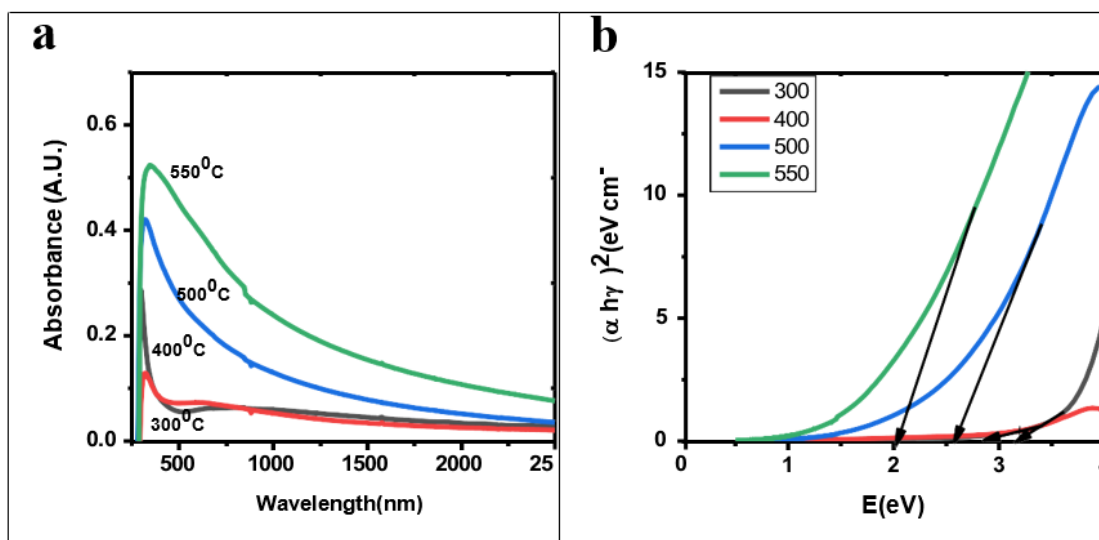


Fig. 4 Absorbance spectra for thin film samples.

#### 4- CONCLUSIONS

Pure  $WO_3$  thin films were deposited onto cleaned glass substrates using spin coating technique at a rate of 2500 rpm for 30 s. The as-deposited films have been annealed at 300 °C, 400 °C, 500 °C, 550 °C and 600 °C for 2 hours. It was found that the crystallite sizes increased with increasing calcination temperatures from 300 °C, 500 °C to 550 °C. The crystalline sizes were 10, 13, 24 and 28 nm respectively. The energy gap estimated from Tauc-plot curve was decreasing with increasing calcined temperature. The energy gap values for the thin film sample calcined at 400 °C is about 2.95, generally consistent with that reported for the  $WO_3$  ( $E_g=2.8$  eV), and it was 2.58, and 2.023 for samples calcined at 500 °C, 550 °C, respectively.

#### 5- REFERENCES

Boulova, M., Gaskov, A., and Lucazeau, G. (2001). Tungsten oxide reactivity versus  $CH_4$ , CO and  $NO_2$  molecules studied by Raman spectroscopy. *Sensors and Actuators B: Chemical*, 81(1), 99–106.

- Chacón, C., Rodríguez-Pérez, M., Oskam, G., and Rodríguez-Gattorno, G. (2015). Synthesis and characterization of WO<sub>3</sub> polymorphs: monoclinic, orthorhombic and hexagonal structures. *Journal of Materials Science: Materials in Electronics*, 26(8), 5526–5531.
- Chang, K.-H., Hu, C.-C., Huang, C.-M., Liu, Y.-L., and Chang, C.-I. (2011). Microwave-assisted hydrothermal synthesis of crystalline WO<sub>3</sub>–WO<sub>3</sub>·0.5 H<sub>2</sub>O mixtures for pseudocapacitors of the asymmetric type. *Journal of Power Sources*, 196(4), 2387–2392.
- Chen, Z., Zhao, J., Yang, X., Ye, Q., Huang, K., Hou, C., and Li, Y. (2016). Fabrication of TiO<sub>2</sub>/WO<sub>3</sub> composite nanofibers by electrospinning and photocatalytic performance of the resultant fabrics. *Industrial & Engineering Chemistry Research*, 55(1), 80–85.
- Çırak, Ç., Kılınç, T., Karadeniz, S. M., Çırak, B. B., and Ekinci, A. E. (2016). Effects of Some Parameters on WO<sub>3</sub> Nanostructures Synthesized by Spin Coating. In *Journal of Engineering Trends and Technology (IJETT) – Volume-40 Number-5*
- Deepa, M., Singh, P., Sharma, S. N., and Agnihotry, S. A. (2006). Effect of humidity on structure and electrochromic properties of sol–gel-derived tungsten oxide films. *Solar Energy Materials and Solar Cells*, 90(16), 2665–2682.
- Garg, D., Henderson, P. B., Hollingsworth, R. E., and Jensen, D. G. (2005). An economic analysis of the deposition of electrochromic WO<sub>3</sub> via sputtering or plasma enhanced chemical vapor deposition. *Materials Science and Engineering: B*, 119(3), 224–231.
- Go, G. H., Shinde, P. S., Doh, C. H., and Lee, W. J. (2016). PVP-assisted synthesis of nanostructured transparent WO<sub>3</sub> thin films for photoelectrochemical water splitting. *Materials & Design*, 90, 1005–1009.
- Işık, D., Ak, M., and Durucan, C. (2009). Structural, electrochemical and optical comparisons of tungsten oxide coatings derived from tungsten powder-based sols. *Thin Solid Films*, 518(1), 104–111.
- Joraid, A. A. (2009). Comparison of electrochromic amorphous and crystalline electron beam deposited WO<sub>3</sub> thin films. *Current Applied Physics*, 9(1), 73–79.
- Kanan, S. M., and Tripp, C. P. (2007). Synthesis, FTIR studies and sensor properties of WO<sub>3</sub> powders. *Current Opinion in Solid State and Materials Science*, 11(1–2), 19–27.
- Liu, Z., Miyauchi, M., Yamazaki, T., & Shen, Y. (2009). Facile synthesis and NO<sub>2</sub> gas sensing of tungsten oxide nanorods assembled microspheres. *Sensors and Actuators B: Chemical*, 140(2), 514–519.
- Ozkan, E., Lee, S.-H., Liu, P., Tracy, C. E., Tepehan, F. Z., Pitts, J. R., and Deb, S. K. (2002). Electrochromic and optical properties of mesoporous tungsten oxide films. *Solid State Ionics*, 149(1–2), 139–146.
- Pal, B., Vijayan, B. L., Krishnan, S. G., Harilal, M., Basirun, W. J., Lowe, A., and Jose, R. (2018). Hydrothermal syntheses of tungsten doped TiO<sub>2</sub> and TiO<sub>2</sub>/WO<sub>3</sub> composite using metal oxide precursors for charge storage applications. *Journal of Alloys and Compounds*, 740, 703–710.
- Patil, P. S., Mujawar, S. H., Inamdar, A. I., and Sadale, S. B. (2005). Electrochromic properties of spray deposited TiO<sub>2</sub>-doped WO<sub>3</sub> thin films. *Applied Surface Science*, 250(1–4), 117–123.

- Riech, I., Acosta, M., Zambrano-Arjona, M. A., Penunuri, F., Rosado-Mendoza, M., Marín, E. and Mendoza-Álvarez, J. G. (2013). Physical properties of macroporous tungsten oxide thin films and their impact on the photocurrent density. *International Journal of Photoenergy*, 2013.
- Saleem, M., Al-Kuhaili, M. F., Durrani, S. M. A., Hendi, A. H. Y., Bakhtiari, I. A., and Ali, S. (2015). Influence of hydrogen annealing on the optoelectronic properties of WO<sub>3</sub> thin films. *International Journal of Hydrogen Energy*, 40(36), 12343–12351.
- Su, L., & Lu, Z. (1998). All solid-state smart window of electrodeposited WO<sub>3</sub> and TiO<sub>2</sub> particulate film with PTREFG gel electrolyte. *Journal of Physics and Chemistry of Solids*, 59(8), 1175–1180.
- Su, X., Li, Y., Jian, J., and Wang, J. (2010). In situ etching WO<sub>3</sub> nanoplates: hydrothermal synthesis, photoluminescence and gas sensor properties. *Materials Research Bulletin*, 45(12), 1960–1963.
- Sun, Y., Murphy, C. J., Reyes-Gil, K. R., Reyes-Garcia, E. A., Thornton, J. M., Morris, N. A., and Raftery, D. (2009). Photoelectrochemical and structural characterization of carbon-doped WO<sub>3</sub> films prepared via spray pyrolysis. *International Journal of Hydrogen Energy*, 34(20), 8476–8484.
- Susanti, D., Haryo, N. S., Nisfu, H., Nugroho, E. P., Purwaningsih, H., Kusuma, G. E., and Shih, S.-J. (2012). Comparison of the morphology and structure of WO<sub>3</sub> nanomaterials synthesized by a sol-gel method followed by calcination or hydrothermal treatment. *Frontiers of Chemical Science and Engineering*, 6(4), 371–380.
- Wang, S.-H., Chou, T.-C., and Liu, C.-C. (2003). Nano-crystalline tungsten oxide NO<sub>2</sub> sensor. *Sensors and Actuators B: Chemical*, 94(3), 343–351.
- Yan, A., Xie, C., Zeng, D., Cai, S., and Hu, M. (2010). Synthesis, formation mechanism and sensing properties of WO<sub>3</sub> hydrate nanowire netted-spheres. *Materials Research Bulletin*, 45(10), 1541–1547.